Long non-coding RNA STARD13-AS suppresses glioma cell biological activities by vitro study

Hua Shan, Yijun Ma, Suijun Zhu

Department of Neurosurgery, Yuhang District First People's Hospital, Hangzhou, China

Corresponding author:
Suijun Zhu
Department of Neurosurgery
Yuhang District
First People's Hospital
Hangzhou, China
E-mail: zhusuijun1215@163.
com

Abstract

Introduction: It has been unclear whether STARD13-AS has effects in glioma. The aim of our research was to investigate the effects of STARD13-AS in glioma development and the mechanisms underlying these effects.
Material and methods: Adjacent normal and tumor tissues were collected for long non-coding RNA (lncRNA) microarray screening. STARD13-AS expression was measured by in situ hybridization (ISH) and reverse-transcription quantitative PCR (RT-qPCR) assays, and correlations between STARD13-AS and clinicopathological parameters and prognosis were analyzed. STARD13-AS transfection of glioma cell lines (U251 and U87) was used to evaluate biological activities of cells. Western blotting (WB) and RT-qPCR assays were used to investigate the underlying mechanisms.
Results: According to lncRNA microarray screening, ISH, and RT-qPCR, lncRNA STARD13-AS was significantly downregulated in tumor tissues. Low STARD13-AS expression was strongly correlated with poor prognosis and malignant clinicopathology. After STARD13-AS transfection, biological activities of glioma cells were significantly decreased ($p < 0.001$ for both cell types). WB and RT-qPCR assays showed that protein and mRNA expression levels of cyclin D, cyclin E, N-cadherin, E-cadherin, and vimentin were significantly related to STARD13-AS overexpression ($p < 0.001$ in all cases).
Conclusions: STARD13-AS overexpression suppresses the biological activities of glioma cells, indicating that STARD13-AS is a potential target for glioma treatment.

Key words: lncRNA STARD13-AS, glioma, U251, U87, cell biological activities.

Introduction

Glioma is a common malignant tumor of the brain that accounts for 45% of intracranial tumors and 80% of intracranial malignant tumors, and has the highest incidence and mortality among malignant tumors of the central nervous system [1]. The boundary between infiltrative glioma cells and normal brain tissue is not clear, and glioma is characterized by high incidence, a short disease course, high mortality, frequent relapse, and a low cure rate [2]. The main treatment for glioma consists of surgery combined with radiotherapy and chemotherapy; this treatment can quickly relieve patients' symptoms, but residual lesions often lead to relapse and the prognosis is poor [3]. Therefore, it is crucial to develop individualized therapeutic schedules and methods of prognosis evalu-

AMS

ation based on genes related to the occurrence and development of glioma. Recent research into targeted therapies based on tumor genetics and molecular mechanisms could provide new approaches to the diagnosis and treatment of glioma. Long non-coding RNAs (lncRNAs) are widely involved in the regulation of multiple biological processes of cells, including proliferation, differentiation, apoptosis, and metabolism [4]. The expression profiles of lncRNAs vary between normal tissues and cancer tissues; this provides a basis for the diagnosis, treatment, and prognosis of various human cancers [5]. StAR-related lipid transfer domain protein 13-antisense RNA (STARD13-AS) is a kind of lncRNA. Previous studies found that lncRNA STARD13-AS over-expression led to suppression of gastric cancer [6], colorectal cancer [7] and lung squamous carcinoma [8]. However, until now, it has been unclear whether lncRNA STARD13-AS has effects in glioma.

In this study, three pairs of cancerous tissues and para-carcinoma tissues from glioma patients were analyzed using cDNA microarrays. STARD13-AS, the lncRNA with the most differential expression, was selected as the research object. Reverse-transcription quantitative PCR (RT-qPCR) and in situ hybridization (ISH) were used to measure STARD13-AS expression in the cancerous tissues and para-carcinoma tissues, and the effects of STARD13-AS on patient prognosis were analyzed using clinical data. To further explore the mechanism of STARD13-AS in glioma, we designed relevant cell experiments to study and analyze its role.

Material and methods

General data

Eighty-two glioma patients admitted to our hospital between April 2013 and April 2016 were selected. The inclusion criteria were as follows: patients were diagnosed with glioma by pathology; and complete clinical data and follow-up records were available. All patients provided signed informed consent, and the study was approved by the ethics committee of Hangzhou Yuhang District First People's Hospital. Exclusion criteria were as follows: non-primary glioma; history of surgery or chemoradiotherapy; severe metabolic disease; other malignant tumors; other central nervous system diseases; history of central nervous system disease injury; and incomplete follow-up. Of the eligible patients, 44 were male and 38 were female. Patient ages ranged from 28 to 72 (55.24 ±4.68) years. Pathological type was astrocytoma in 35 cases, anaplasia astrocytoma in 21 cases, glioblastoma in 16 cases, and oligodendroglia astrocytoma in 10 cases. The World Health Organization

(WHO) classification [9] was I–II in 35 cases and III–IV in 47 cases; and the Karnofsky performance score (KPS) was ≤ 80 points in 37 cases and > 80 points in 45 cases. This study was approved by the Ethics Committee of Hangzhou Yuhang District First People's Hospital (No. YHEC2012120612), and all patients signed informed consent.

Follow-up visits

Patients were followed up by monthly telephone inquiries until 31 March 2019.

Materials and reagents

Normal human glial cells (HEB cells) and human glioma cell lines (U251, U87, LN-18, H4, and M059K) were purchased from ATCC; DMEM culture medium was purchased from Zhejiang Tianhang Biotechnology Co., Ltd.; pcDNA3.1 and related transfection agents were purchased from Invitrogen; anti-cyclin D, cyclin E, N-cadherin, vimentin, E-cadherin, and GAPDH were purchased from Jiangsu Beyotime Institute of Biotechnology; the CCK-8 kit was from Guangzhou Laide Biotechnology Co., Ltd. (Guangzhou, China); and the apoptosis and cycle detection kit was from KeyGen Biotech (Nanjing, China). lncRNA STARD13-AS and SYBR Green I real were also used.

lncRNA microarray screening

Three pairs of tissues (normal tissue and cancer tissue) were selected for microarray detection and analysis by Shanghai GeneChem Co., Ltd.

ISH detection

Tissue samples were embedded in paraffin. Embedded sections were incubated with HCl at room temperature for 5 min and washed with phosphate-buffered saline (PBS) three times, 5 min per time. Sections were incubated first with protease K for 20 min, followed by washing three times with PBS, 5 min per time; then with polyformaldehyde for 10 min, followed by washing twice with PBS, 5 min per time; and finally with acetic anhydride and triethanolamine solution for 10 min at room temperature, followed by washing three times with PBS, 5 min per time. The probe was diluted with hybridization solution and denatured at 85°C for 5 min. It was then added to the tissue samples, sealed overnight at 37°C, and washed twice in saline-sodium citrate (SSC) buffer, 20 min per time, before being rinsed three times with formamide/SSC buffer at 37°C, 20 min per time, and finally rinsed with TBST (Tris-buffered saline, 0.1% Tween 20) five times for 10 min per time. Samples were blocked with 3% bovine serum albumin at room temperature for 1 h, in-

cubated overnight at 4°C with anti-digoxin I antibody (1 : 1000), then washed four times with TBST, 10 min per time, and twice with BCIP/NBT dye buffer, 10 min per time. Samples were stained in the dark with BCIP/NBT for 4–48 h, followed by washing twice with TE buffer (pH 8.0) to stop the reaction. Finally, samples were washed to remove residue, dehydrated, and blocked, before being observed under an inverted microscope and photographed. The Image J image analysis software was used to determine STARD13-AS expression in each section.

RT-qPCR detection

Total RNA was extracted by the TRIzol method (Invitrogen, CA, USA) from tissues or cells, and quantified using an absorbance ratio of 1.9-2.0. One microliter of total RNA was taken and reverse-transcribed into cDNA according to the reverse-transcription kit instructions. Then, real-time quantitative RT-PCR was used to detect the expression level of the target gene, with GAPDH as an internal reference. Primer sequences are structured from KeyGEN Bio Tech (Nanjing, China) and shown in Table I. The quantitative analysis used the $2^{-\Delta\Delta Ct}$ method. All experiments were repeated at least three times.

Cell culture

HEB, U251, U87, LN-18, H4, and M059K cells were cultured in DMEM containing 10% fetal bovine serum in an incubator at 37°C and 5% CO_2. The culture solution was changed every 2 days, with passage of 3–5 days. Cell transfection was carried out according to the instructions. Cells in the logarithmic growth phase were inoculated into six-well plates. Once the cells were fused to 60%, the medium was changed to a serum-free medium and synchronized for 12 h, followed by transfection. The groups comprised a normal control group (NC), blank transfection group (pcDNA3.1), and STARD13-AS group. Cells in the NC group were cultured routinely; those in the pcDNA3.1 group were transfected with a pcDNA3.1 empty vector; and those in the STARD13-AS group were transfected with Lipofectamine 2000 (Invitrogen, Carlsbad, CA, USA). The subsequent experiments were conducted at least 24 h after transfection.

Detection of cell reproductive capacity by CCK-8

Cells were inoculated in 96-well plates (1 × 10^4 per well) and cultured after the appropriate treatment. CCK-8 reagent was added to each well 2 h before the end of culture. The absorbance at 450 nm of each well was determined. For each group, the mean value of three multiple wells was recorded. Medium alone was added to a single well as a blank control.

Cell apoptosis and cycle by flow cytometry assay

Cell apoptosis was detected using an Annexin V–FITC/PI double staining kit. Cells in the logarithmic growth phase were inoculated in six-well plates (4 × 10^5 cells per well) and cultured for 24 h. The medium was then discarded. After treatment, cells in each group were cultured for another 48 h and then collected. The experiment was conducted according to the kit instructions. Apoptosis and cell cycling in each group were detected and analyzed by flow cytometry.

Detection of cell migration and invasion by transwell assay

Cells were collected from each group and resuspended in culture medium to adjust the cell density to 2 × 10^8/l. Cells were inoculated in the upper compartment of the transwell chamber, and complete culture medium was added to the lower compartment, followed by incubation for 6 h. After removal from the incubator, cells on the surface of the upper compartment were rinsed and erased with PBS. Cells in the transwell chamber were fixed with 90% ethanol followed by addition of 0.1% crystal violet dye. After rinsing with PBS again, the number of stained cells was counted under an inverted microscope (the mean value of three visual fields was taken for each group).

Wound healing assays

Cell migration was detected by cell wound healing assays. Cells in each group were treated

Table I. Primers for RT-PCR

Gene name	Primer sequence
STARD13-AS	F: 5'-CCACAGAGAGGATTCCAGAA-3'
	R: 5'-TCCAGGCTCTGTATAGAAGCT-3'
Cyclin D	F:5'-GTAGCAGCCAGCAGCAGAGT-3'
	R:5'-CTCCTCGCACTTCTGTTCCTC-3'
Cyclin E	F: 5'-CTCCAGGAAGAGGAAGGCAA-3'
	R: 5'-TCGATTTTGGCCATTTCTTCA-3'
N-cadherin	F:5'-GCTTATCCTTGTGCTGATGTTT-3'
	R: 5'-GTCTTCTTCTCCTCCACCTTCT-3'
E-cadherin	F: 5'-CTCACATTTCCCAACTCCTCT-3'
	R: 5'-TGTCACCTTCAGCCATCCT-3'
Vimentin	F: 5'-CTGTGGCATCCACGAAACT-3'
	R: 5'-CGGACTCGTCATACTCCTGCT-3'
GAPDH	F: 5'-GAAGGTCGGAGTCAACGGAT-3'
	R: 5'-CCTGGAAGATGGTGATGGG-3'

by different treatment of every group for 24 h, after which cells in the logarithmic growth phase were taken and inoculated in six-well plates. When the cell density reached 80%, the cell layers were scratched with pipette tips, then washed with PBS and cultured for 24 h or 48 h, before being observed and photographed under a microscope. The wound healing rate was calculated for each group as wound healing rate = (0 h length − 24 h or 48 h length)/0 h length × 100%.

Determination of protein level by WB

Cellular proteins were extracted by RIPA pyrolysis and quantified using a BCA kit, followed by sodium dodecyl sulfate polyacrylamide gel electrophoresis. The total quantity of loading protein was adjusted to 60 μg, and protein loading buffer was added in a 1 : 4 volume ratio. Electrophoresis was performed after denaturation of samples at 100°C. Proteins were then transferred onto polyvinylidene fluoride membranes. After blocking with 5% skim milk at room temperature for 90 min, the corresponding proportion of primary antibody was added, followed by incubation overnight at 4°C according to the instructions and washing with TBST three times for 5 min per time. The corresponding secondary antibody was added, followed by incubation at room temperature for 2 h and washing with TBST three times for 10 min per time. Finally, bands corresponding to proteins were quantified using enhanced chemiluminescence (Keygentec) and ChemiDoc XRS systems (Bio-Rad).

Ethics approval and informed consent

This study was approved by the Ethics Committee of Hangzhou Yuhang District First People's Hospital (approval no. 2012122808) and was conducted in accordance with the Declaration of Helsinki. Written informed consent was obtained from all the participants regarding the use of clinical samples for study purposes.

Statistical analysis

Experimental data were processed using the SPSS 17.0 statistical software. The measurement data followed a normal distribution after the normality test, and are reported as mean ± standard deviation (SD). One-way analysis of variance (Student-Newman-Keuls method for pairwise comparison) was used for multi-group comparisons, and t-tests were used for comparisons between two groups. Counting cell counts are reported as ratios (%) and were analyzed by the χ^2 test. Survival times were analyzed by the Kaplan-Meier method. $P < 0.05$ was considered statistically significant.

Results

lncRNA STARD13-AS expression and its relationship with the prognosis of glioma patients

The microarray results showed that STARD13-AS expression in cancerous tissue was significantly lower than that in adjacent normal tissues (Figure 1 A). RT-qPCR detection in different pathological tissues showed that the expression level of lncRNA STARD13-AS mRNA was significantly lower compared with adjacent normal tissues ($p < 0.01$ and $p < 0.001$, Figure 1 B) and decreased with increasing clinical stage (Figure 1 B). ISH was used to further verify the expression of STARD13-AS in para-cancerous normal tissues at different stages. As shown in Figure 1 C, lncRNA STARD13-AS was expressed in the cytoplasm. Its expression level was significantly lower ($p < 0.01$ and $p < 0.001$, Figure 1 C) compared with para-cancerous normal tissues, and decreased with increasing clinical stage. Glioma patients were divided into low- and high-expression groups based on the median mRNA expression level in glioma tissues. Survival analysis showed that patients in the STARD13-AS high-expression group had significantly better overall survival and progression-free survival than those in the STARD13-AS low-expression group ($p = 0.0019$ and $p = 0.0021$, respectively; Figures 1 D, E).

Expression of lncRNA STARD13-AS and its relationship with clinicopathological parameters

Patients were assigned to either the high-expression group ($n = 38$) or the low-expression group ($n = 44$) on the basis of the mean expression level of lncRNA STARD13-AS in glioma tissues 0.32-fold. STARD13-AS was related to WHO grade, KPS, tumor diameter, and number of invaded lobes ($p < 0.05$) but was not related to the age or sex of patients ($p > 0.05$). Details are shown in Table II.
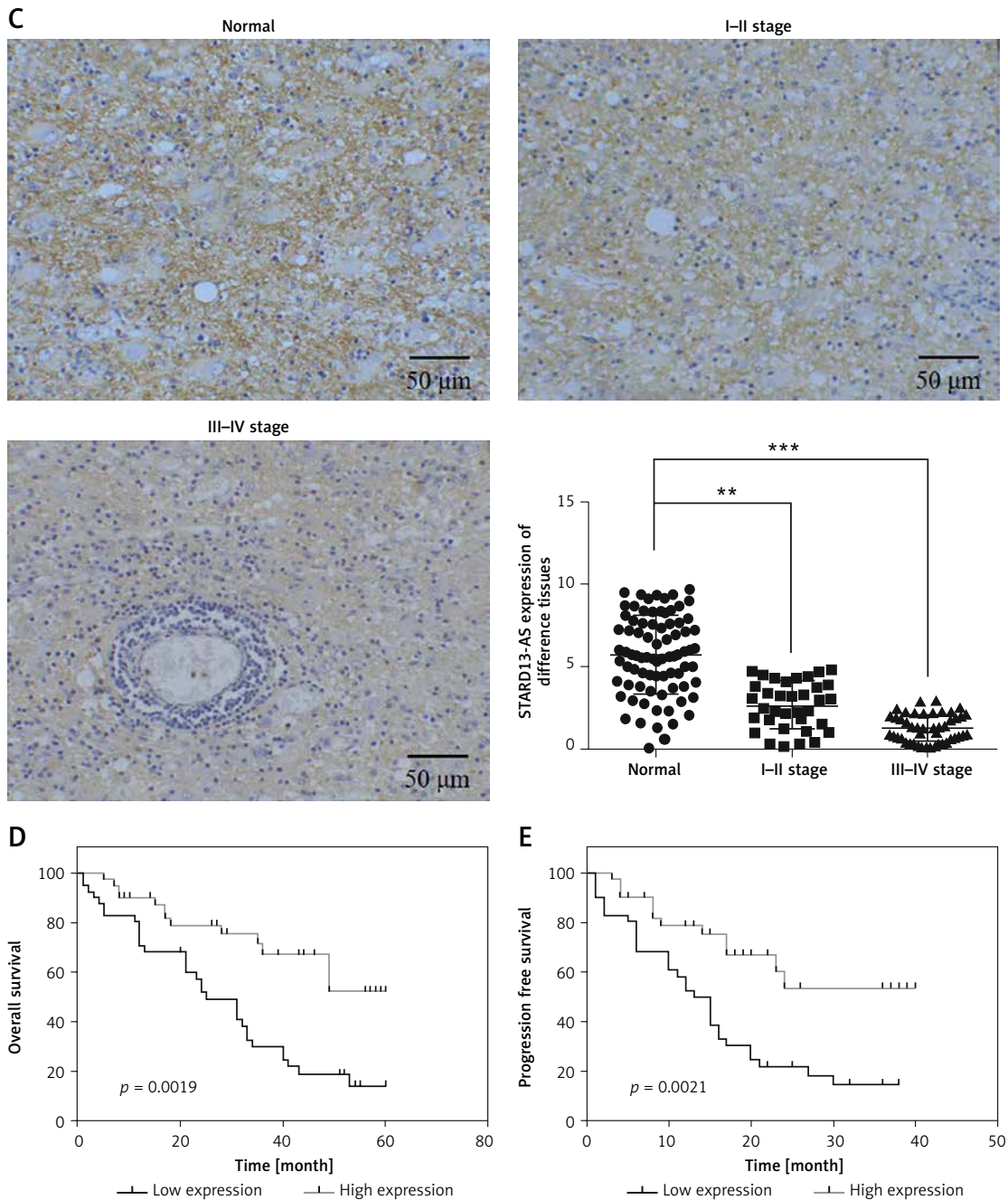
STARD13-AS mRNA expression in different cells and groups, and its effects on cell proliferation

The RT-qPCR results showed that STARD13-AS mRNA expression was significantly downregulated in the glioma cell lines compared with normal human glial (HEB) cells ($p < 0.001$ in all cases, Figure 2 A). The lowest STARD13-AS mRNA levels were found in the U87 and U251 cell lines. Compared with the NC group, the STARD13-AS transfection group showed significantly higher STARD13-AS mRNA levels in both the U251 and U87 cell lines ($p < 0.001$ in both cases, Figure 2 B). The CCK-8 assay results showed that cell proliferation rates were significantly lower compared with the
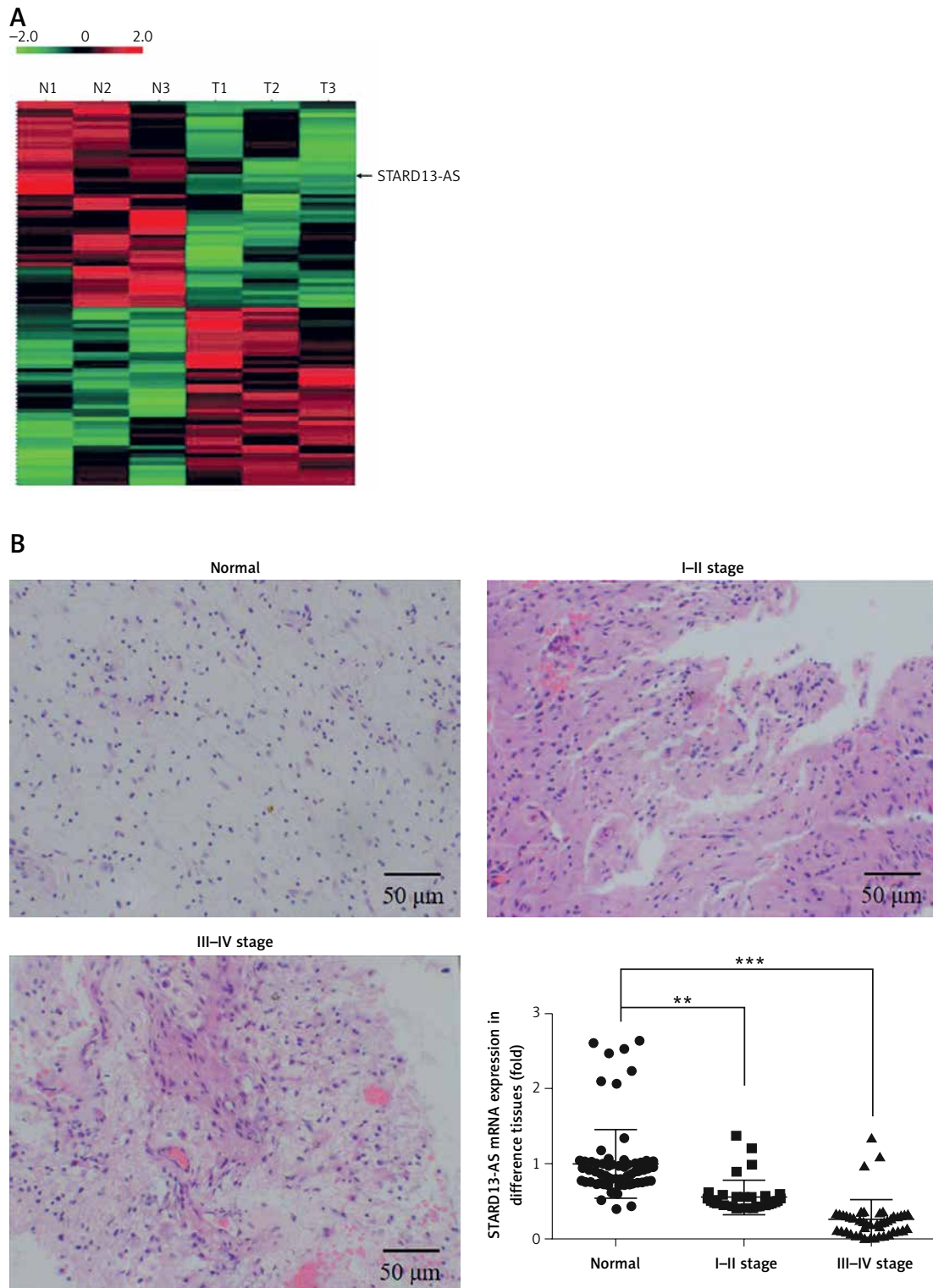
Figure 1. lncRNA STARD13-AS expression and its relationship with prognosis of glioma patients. **A** – Heat map of glioma patients lncRNA expression: N, adjacent normal tissues (which was more than 5 cm from cancer tissues); T, tumor tissues. **B** – Pathology by hematoxylin and eosin staining (200×) and STARD13-AS mRNA by RT-qPCR assay in different tissues

**P < 0.01, ***P < 0.001 vs. normal.

C

Figure 1. Cont. **C** – STARD13-AS expression in different tissues by ISH assay (200×). **D** – Overall survival in different STARD13-AS expression groups. **E** – Progression-free survival in different STARD13-AS expression groups

**P < 0.01, ***P < 0.001 vs. normal.

NC groups in both the U251 and U87 cell lines ($p < 0.001$ in both cases, Figure 2 C).

Effects of STARD13-AS on apoptosis and cell cycle in U251 and U87 cell lines

Flow cytometry results showed that STARD13-AS overexpression significantly increased ($p < 0.001$, Figures 3 A, B) with G1 phase rate significantly increasing and decreased the G2 phase rate in U251 and U87 cell lines ($p < 0.001$, respectively, Figures 3 C, D).

Effects of STARD13-AS on cell invasion ability

In order to determine the effects of STARD13-AS on cell invasion ability, invasive cell numbers were measured in the different groups by transwell assay. The results showed significantly lower invasive cell numbers in the STARD13-AS groups compared with the NC groups in both the U251 and U87 cell lines ($p < 0.001$ in all cases, Figures 4 A, B).

Table II. Relationship between lncRNA STARD13-AS expression and clinical pathological parameters of glioma

Pathological parameters	n	lncRNA STARD13-AS		χ^2	P-value
		Low expression (n = 44)	High expression (n = 38)		
Age [years]:				0.345	0.557
< 50	36	18 (50.00)	18 (50.00)		
≥ 50	46	26 (56.52)	20 (43.48)		
Sex:				0.030	0.682
Male	44	24 (54.55)	20 (45.45)		
Female	38	20 (52.63)	18 (47.37)		
Tumor size [cm]:				4.156	0.025
< 4	37	14 (37.84)	23 (62.16)		
≥ 4	45	30 (66.67)	15 (33.33)		
WHO stage:				9.216	0.002
I–II	35	12 (34.29)	28 (65.71)		
III–IV	47	32 (68.09)	15 (31.91)		
KPS score:				4.666	0.031
≤ 80	37	15 (40.54)	22 (56.46)		
> 80	45	29 (64.44)	16 (35.56)		
Number of lobes involved (n):				3.952	0.043
< 2	59	28 (47.46)	31 (52.54)		
≥ 2	23	16 (69.57)	7 (30.43)		

Effects of STARD13-AS on cell migration ability

In order to evaluate the effects of STARD13-AS on cell migration, the wound healing rates of different groups were analyzed over 24 h and 48 h. Compared with the NC group, wound healing rates were significantly lower in the STARD13-AS groups, over both 24 h and 48 h, in both the U251 and U87 cell lines ($p < 0.001$ in all cases, Figures 5 A, B).

Effects of STARD13-AS on relative protein expression

WB assays were used to determine how STARD13-AS affects relative protein expression. Compared with the NC group, protein expression levels of cyclin D, cyclin E, N-cadherin, and vimentin were significantly lower, and E-cadherin protein expression was significantly higher, as a result of STARD13-AS overexpression ($p < 0.001$ in all cases, Figures 6 A, B).

Effects of STARD13-AS on relative RNA expression

RT-qPCR assays were used to determine how STARD13-AS affects relative mRNA expression. Compared with the NC group, cyclin D, cyclin E, N-cadherin, and vimentin mRNA expression levels were significantly lower and E-cadherin mRNA expression was significantly higher as a result of

STARD13-AS overexpression ($p < 0.001$ in all cases, Figures 7 A, B).

Discussion

Formerly regarded as "junk" genes, lncRNAs have been confirmed by a large number of studies in recent years to have complex biological functions. They are involved in cell proliferation, apoptosis, differentiation, and disease occurrence via inhibiting mRNA reduction, regulating protein activity, and changing relevant protein-coding genes expression [10–12]. It has been reported that lncRNAs have key roles in the development of glioma. Wang et al. [13] found that overexpression of lncRNA HOXA11-AS in glioma could promote the proliferation of tumor cells, whereas its gene knockdown inhibited cell proliferation by regulating cell cycle progression, and was closely related to glioma grade and prognosis. Gao et al. [14] found that lncRNA HOXA11-AS was highly expressed in both glioma tissues and cell lines, and that the inhibition of lncRNA ZFAS1 in vitro could significantly inhibit proliferation, migration, and invasion of glioma cells, and participated in the carcinogenic process by regulating epithelial-mesenchymal transformation (EMT) and the Notch signaling pathway. STARD13-AS is a recently discovered lncRNA. Previous studies have reported abnormal expression of STARD13-AS in some tumors [15]. Here, microarray, RT-qPCR, and

Hua Shan, Yijun Ma, Suijun Zhu
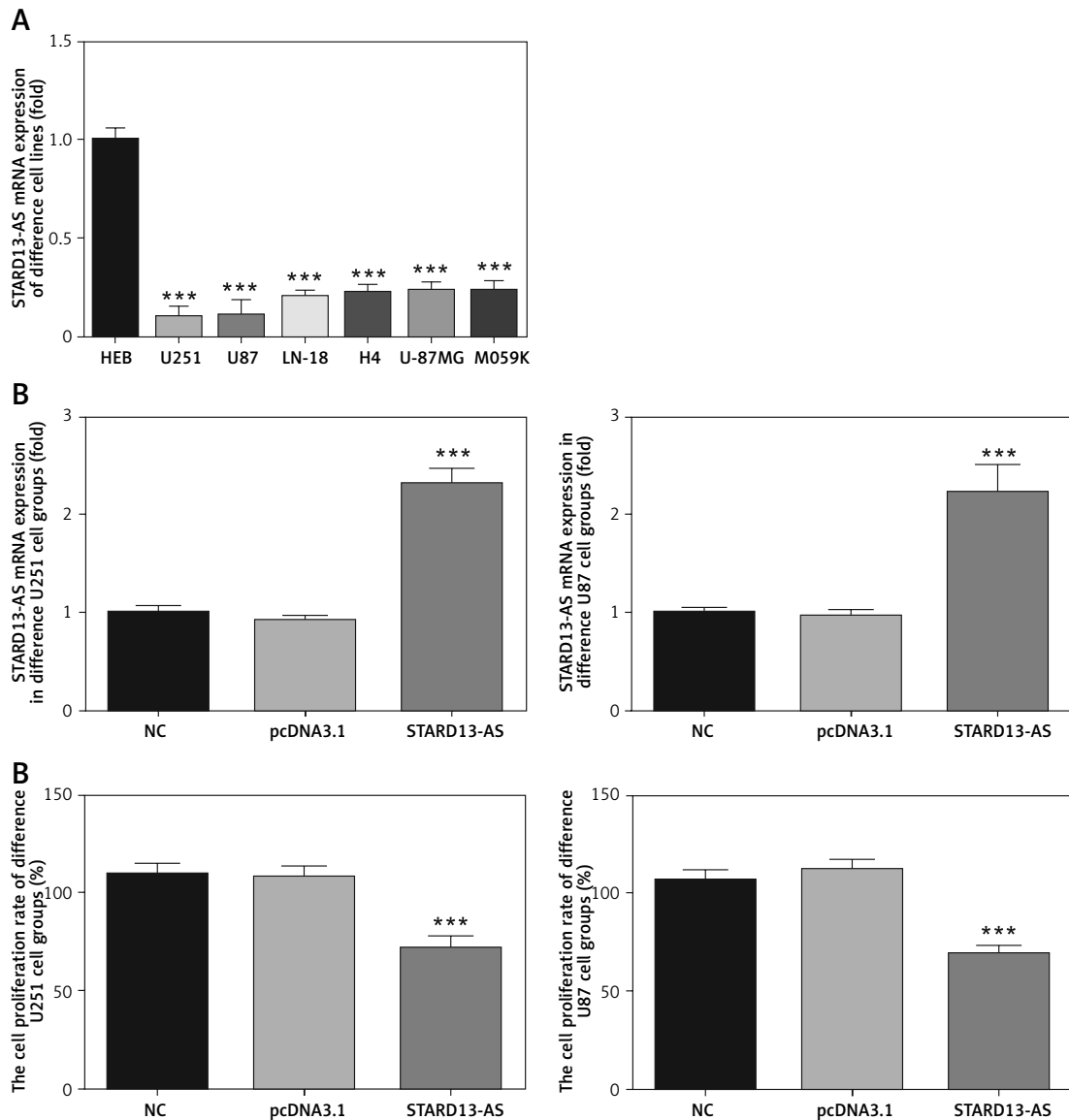
Figure 2. STARD13-AS mRNA expression in different cells and groups, and effects on cell proliferation. **A** – STARD13-AS mRNA expression in different cell lines by RT-qPCR assay (***$p < 0.001$ vs. HEB cell line). **B** – STARD13-AS mRNA expression in different cell groups by RT-qPCR assay (***$p < 0.001$ vs. NC group). **C** – Cell proliferation in different groups by CCK-8 assay (***$p < 0.001$ vs. NC group)

ISH experiments showed that the expression of STARD13-AS in glioma tissues was significantly lower than that in adjacent normal tissues. Survival analysis showed that expression levels of lncRNA STARD13-AS were correlated with WHO grading, KPS, tumor diameter, and number of invaded cerebral lobes, and that the prognosis of patients with low expression of lncRNA STARD13-AS was poor. In order to further explore the mechanism of lncRNA STARD13-AS in glioma, cell experiments were conducted. After transfection of STARD13-AS into cells, proliferation, invasion, and migration of glioma cells were all significantly inhibited, and the apoptosis rate was significantly increased.

The cell cycle has a key role in cell proliferation and apoptosis. Cyclin D and cyclin E are important

proteins in the cell cycle, and their abnormal expression is strongly correlated with tumor development [16, 17]. The present study showed that overexpression of STARD13-AS could effectively inhibit expression of cyclin D and cyclin E in glioma cell lines U251 and U87. Therefore, the results confirmed that the overexpression of STARD13-AS could inhibit the proliferation of glioma cells via effects on the cell cycle. Tumor metastasis is a multi-step process, during which EMT enhances the activity and invasiveness of tumor cells [18, 19]. The first step in the EMT process is to inhibit E-cadherin, thereby reducing cell adhesion [20]. Another important aspect of EMT is upregulated expression of non-epithelial cadherins (including N-cadherin and vimentin) [21, 22]. The results
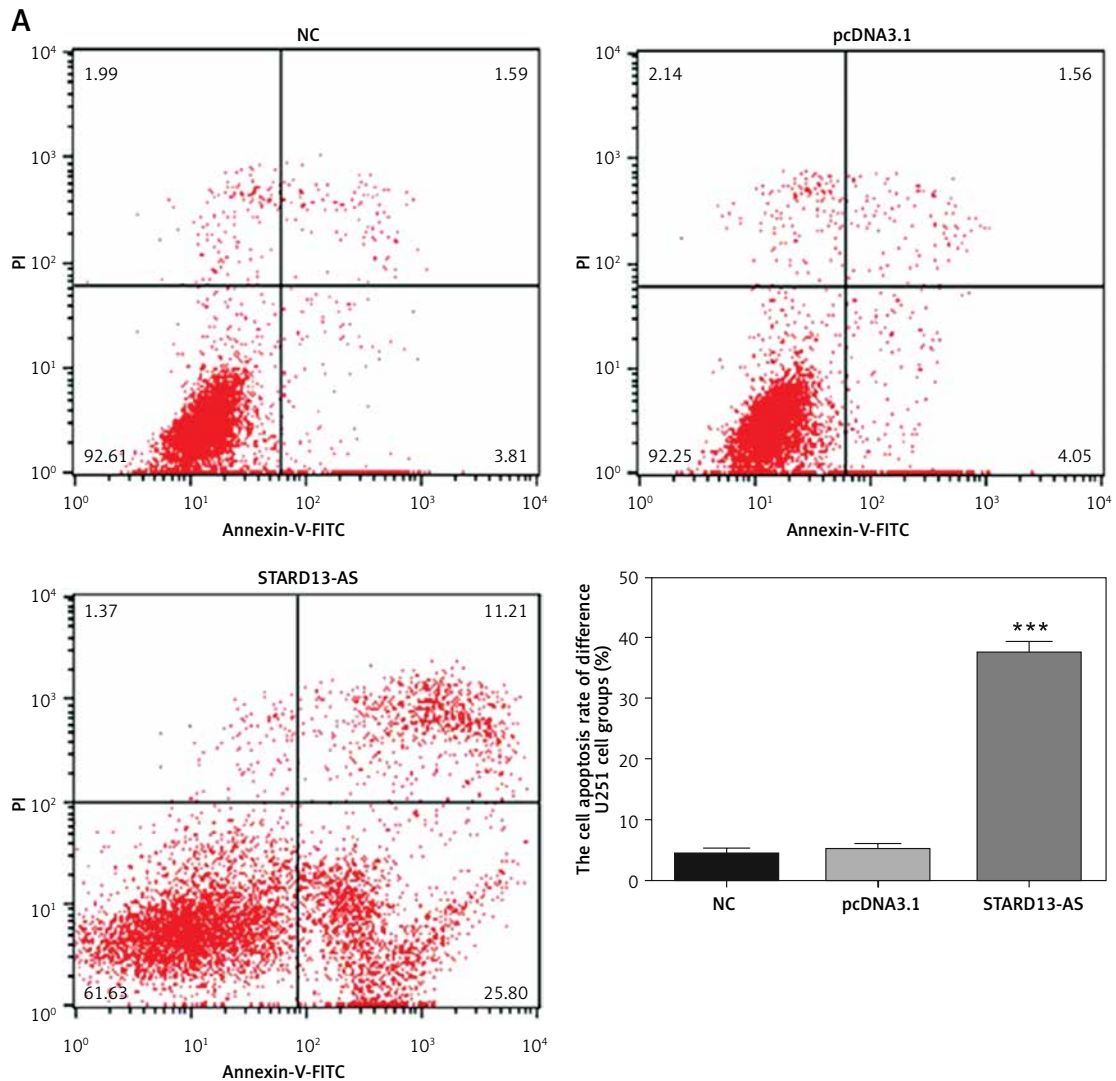
Figure 3. Effects of STARD13-AS on apoptosis and cell cycle in U251 and U87 cell lines. **A** – Effects of STARD13-AS on cell apoptosis by flow cytometry in U251 cell line

***P < 0.001 vs. NC group. NC – no treatment; pcDNA3.1 – cells transfected with empty pcDNA3.1; STARD13-AS – cells transfected with lncRNA STARD13-AS.

showed that high expression of STARD13-AS could increase the expression of E-cadherin in U251 and U87 cells and decrease the expression of vimentin and N-cadherin, thus inhibiting tumor metastasis.

However, the present study had some limitations. First, although high expression of STARD13-AS significantly inhibited proliferation and metastasis of glioma cells in vitro, the specific way in which STARD13-AS affected the proliferation and EMT processes remained unclear and needs further investigation. The target gene of STARD13-AS should be identified in order to further elucidate the underlying mechanism. STARD13-AS is the antisense RNA that encodes RNA-STARD13; thus, we predict that STARD13 might be the target gene of STARD13-AS. Second, animal models are required to verify the effects of overexpression of STARD13-AS on glioma development. We will carry out further experiments to remedy these limitations.

In conclusion, this study confirmed that the expression of lncRNA STARD13-AS in glioma cell lines and tissues was significantly reduced, and that overexpression of STARD13-AS could inhibit proliferation and metastasis of glioma cells. Therefore, STARD13-AS represents a potential target for glioma treatment.
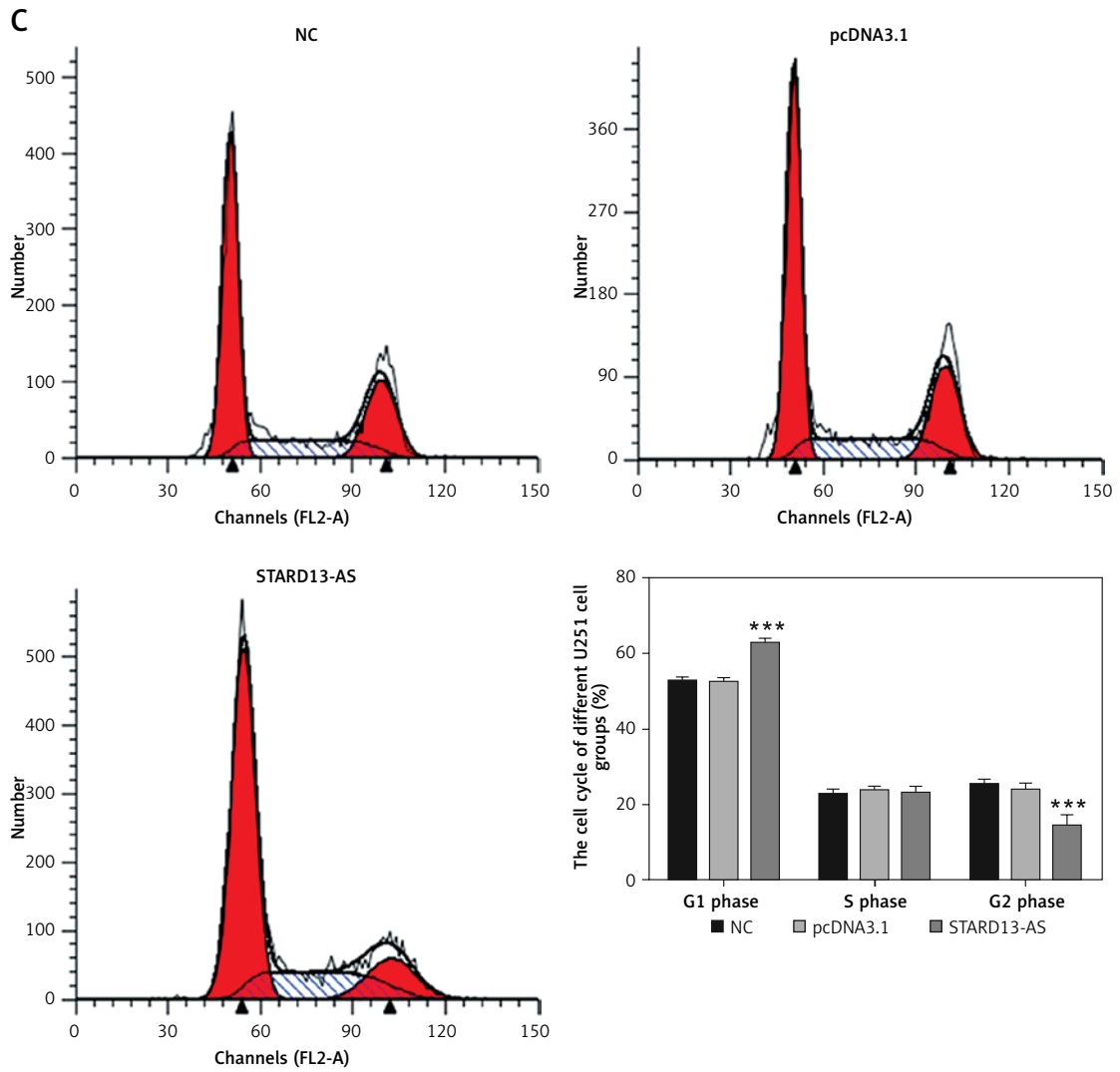
## Conflict of interest

The authors declare no conflict of interest.

B
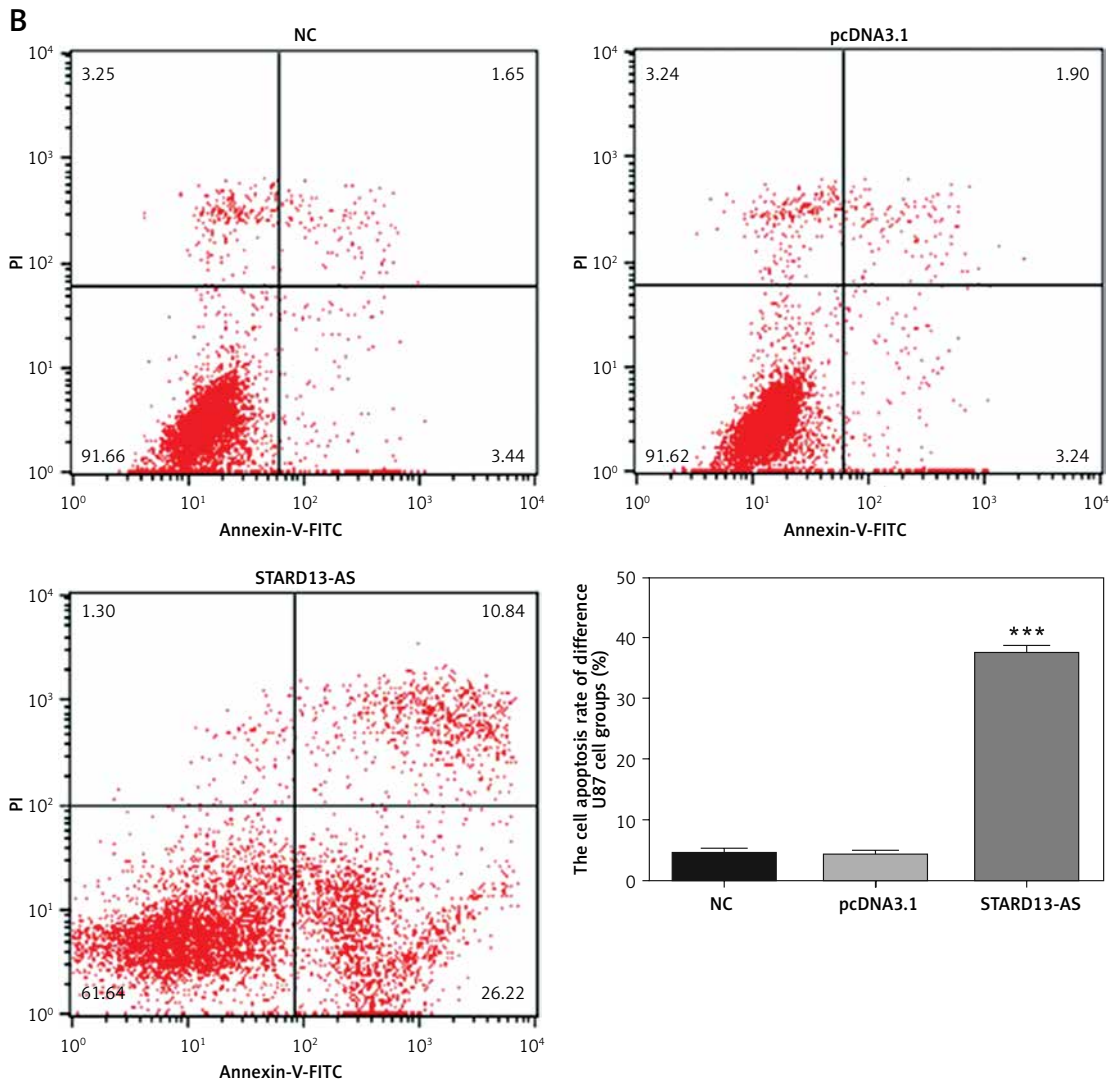
Figure 3. Cont. **B** – Effects of STARD13-AS on cell apoptosis by flow cytometry in U87 cell line

***P < 0.001 vs. NC group. NC – no treatment; pcDNA3.1 – cells transfected with empty pcDNA3.1; STARD13-AS – cells transfected with lncRNA STARD13-AS.
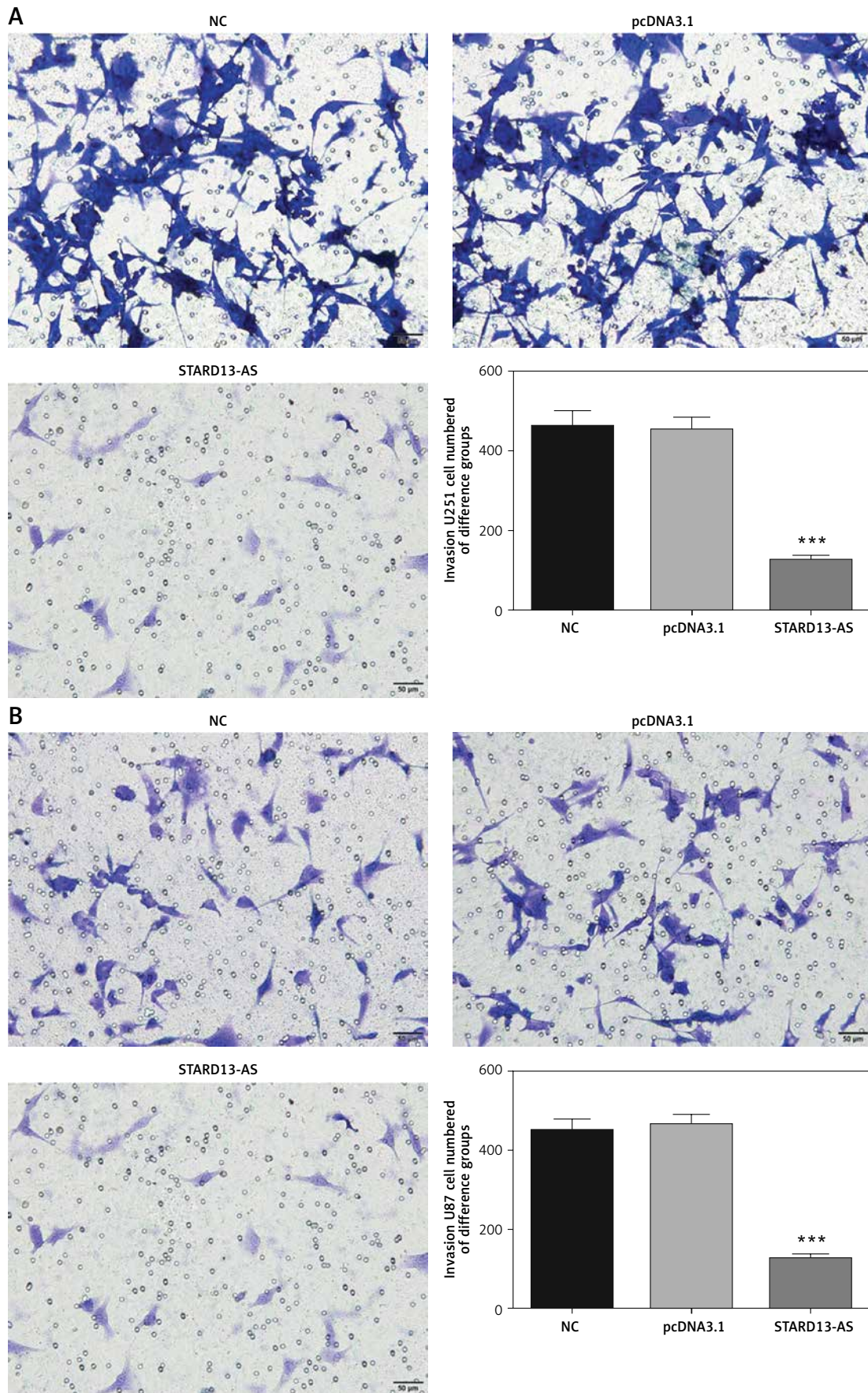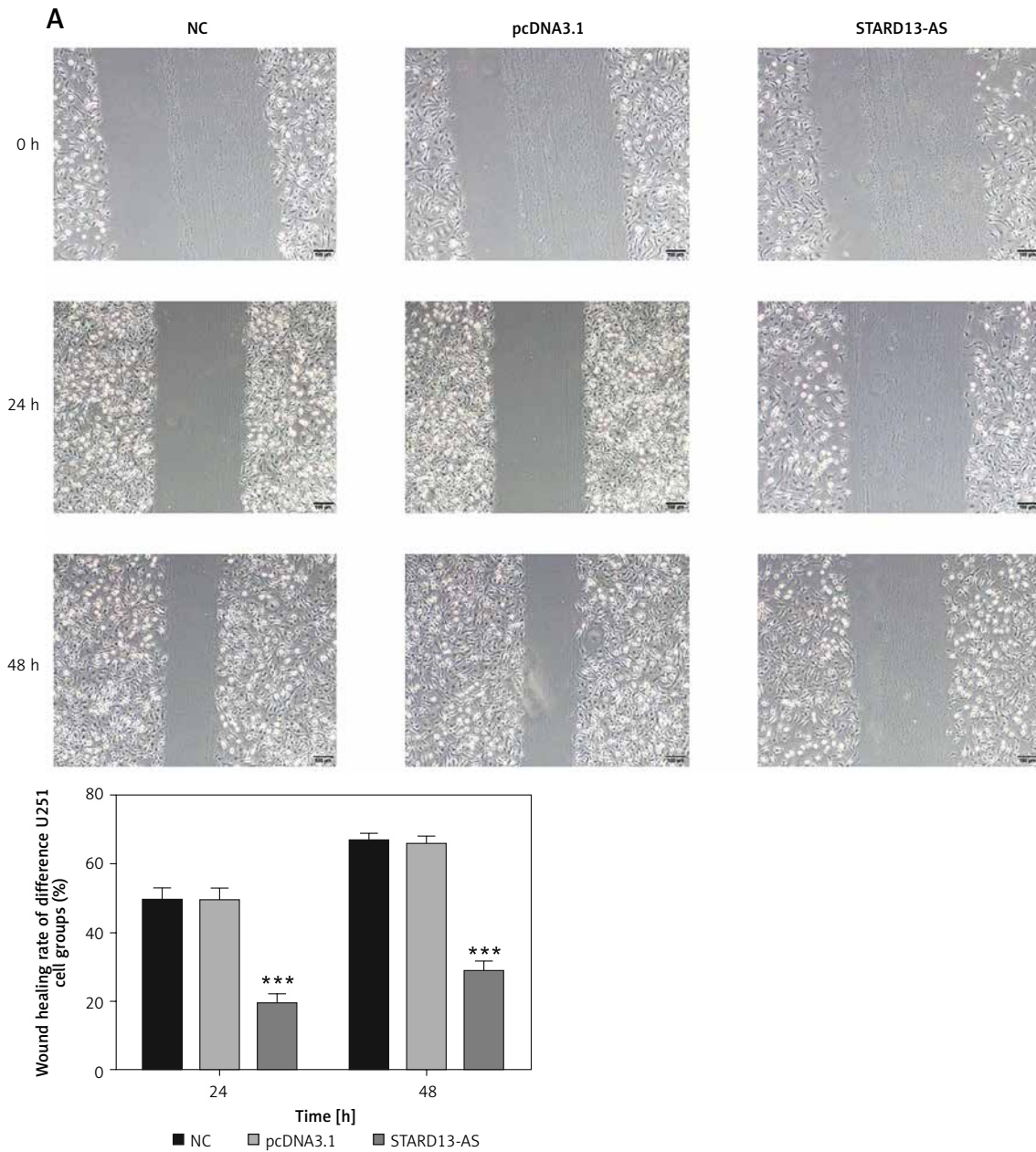
C

Figure 3. Cont. **C** – Effects of STARD13-AS on cell cycle by flow cytometry in U251 cell line

***P < 0.001 vs. NC group. NC – no treatment; pcDNA3.1 – cells transfected with empty pcDNA3.1; STARD13-AS – cells transfected with lncRNA STARD13-AS.

D
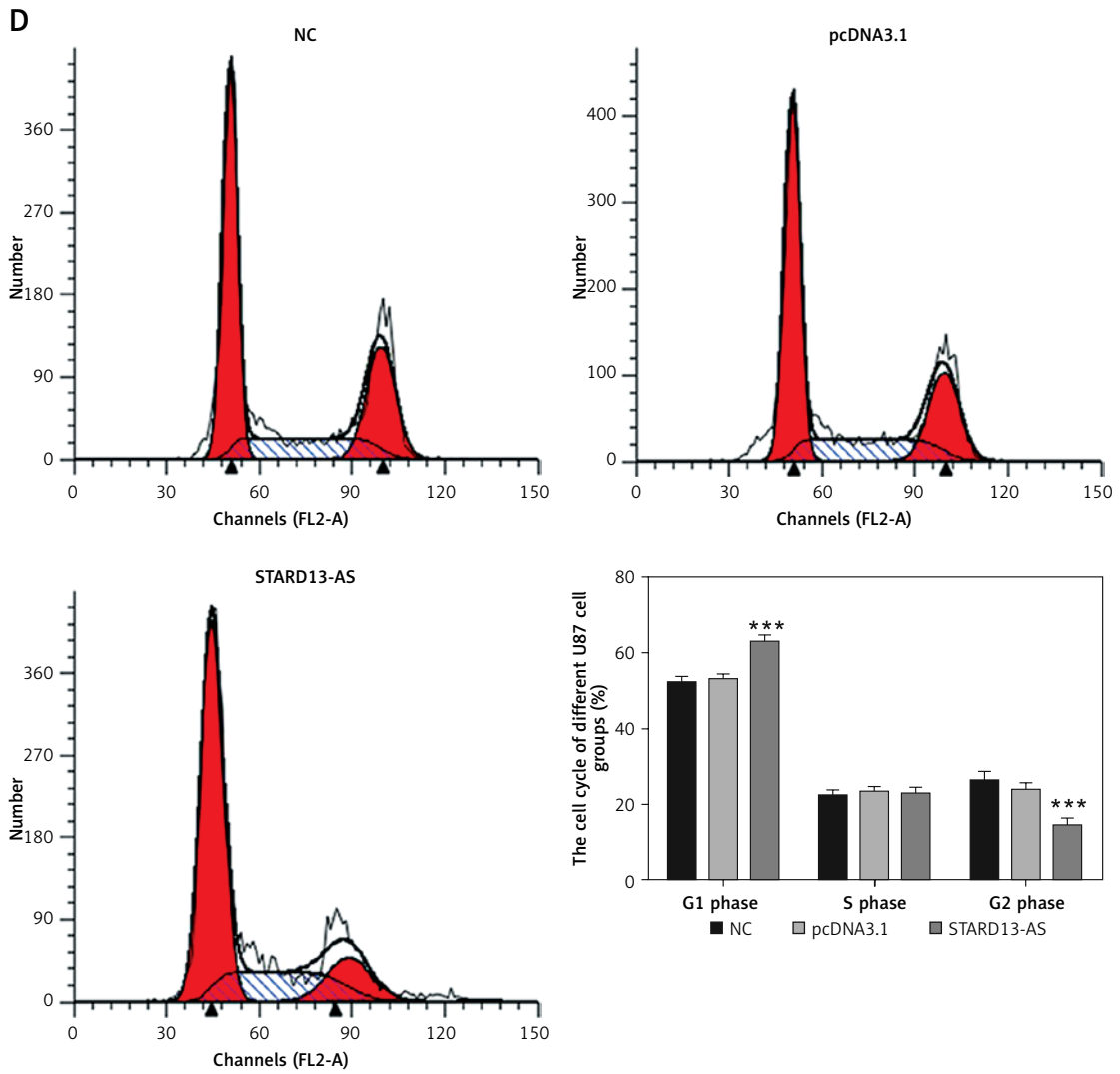
Figure 3. Cont. **D** – Effects of STARD13-AS on cell cycle by flow cytometry in U87 cell line

***P < 0.001 vs. NC group. NC – no treatment; pcDNA3.1 – cells transfected with empty pcDNA3.1; STARD13-AS – cells transfected with lncRNA STARD13-AS.

Figure 4. Effects of STARD13-AS on cell invasion ability by transwell assay (200×). **A** – Numbers of invasive U251 cells in different groups. **B** – Numbers of invasive U87 cells in different groups

***P < 0.001 vs. NC group. NC – no treatment; pcDNA3.1 – cells transfected with empty pcDNA3.1; STARD13-AS – cells transfected with lncRNA STARD13-AS.

Figure 5. Effects of STARD13-AS on cell migration ability by wound healing assay (100×). **A** – Wound healing rates in different U251 cell groups

***P < 0.001 vs. NC group. NC – no treatment; pcDNA3.1 – cells transfected with empty pcDNA3.1; STARD13-AS – cells transfected with lncRNA STARD13-AS.
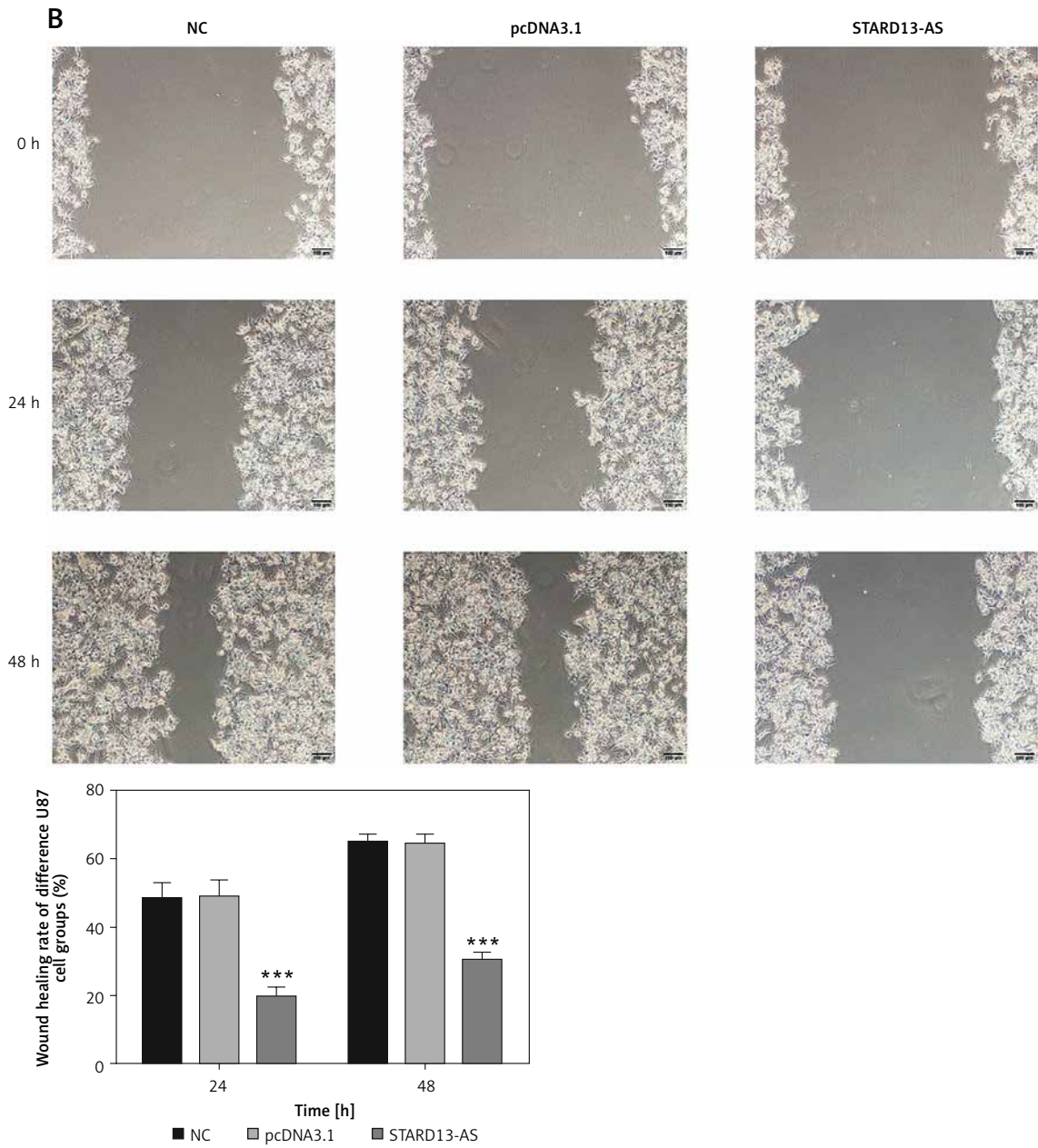
Figure 5. Cont. **B** – Wound healing rates in different U87 cell groups

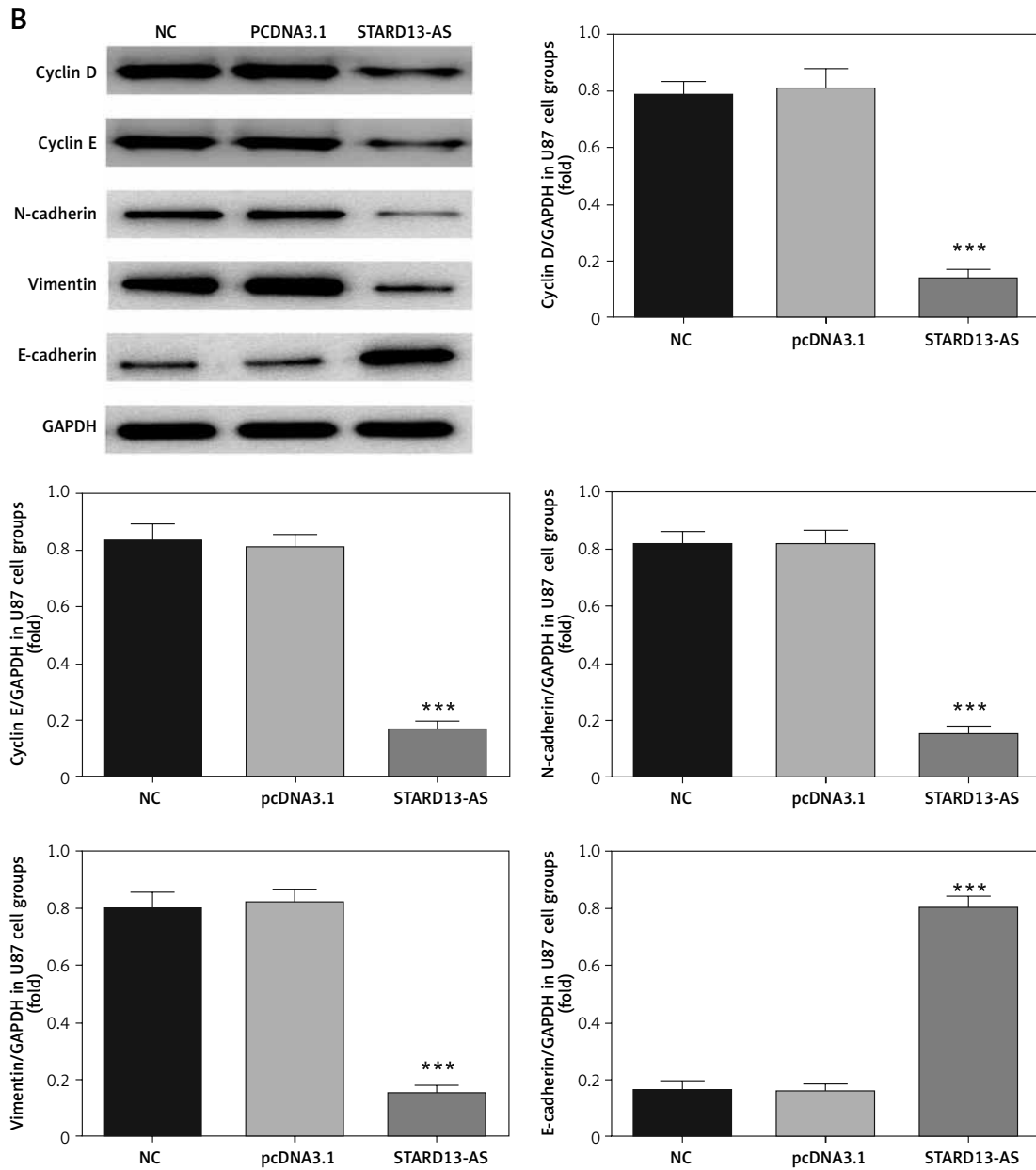****P < 0.001 vs. NC group. NC – no treatment; pcDNA3.1 – cells transfected with empty pcDNA3.1; STARD13-AS – cells transfected with lncRNA STARD13-AS.*
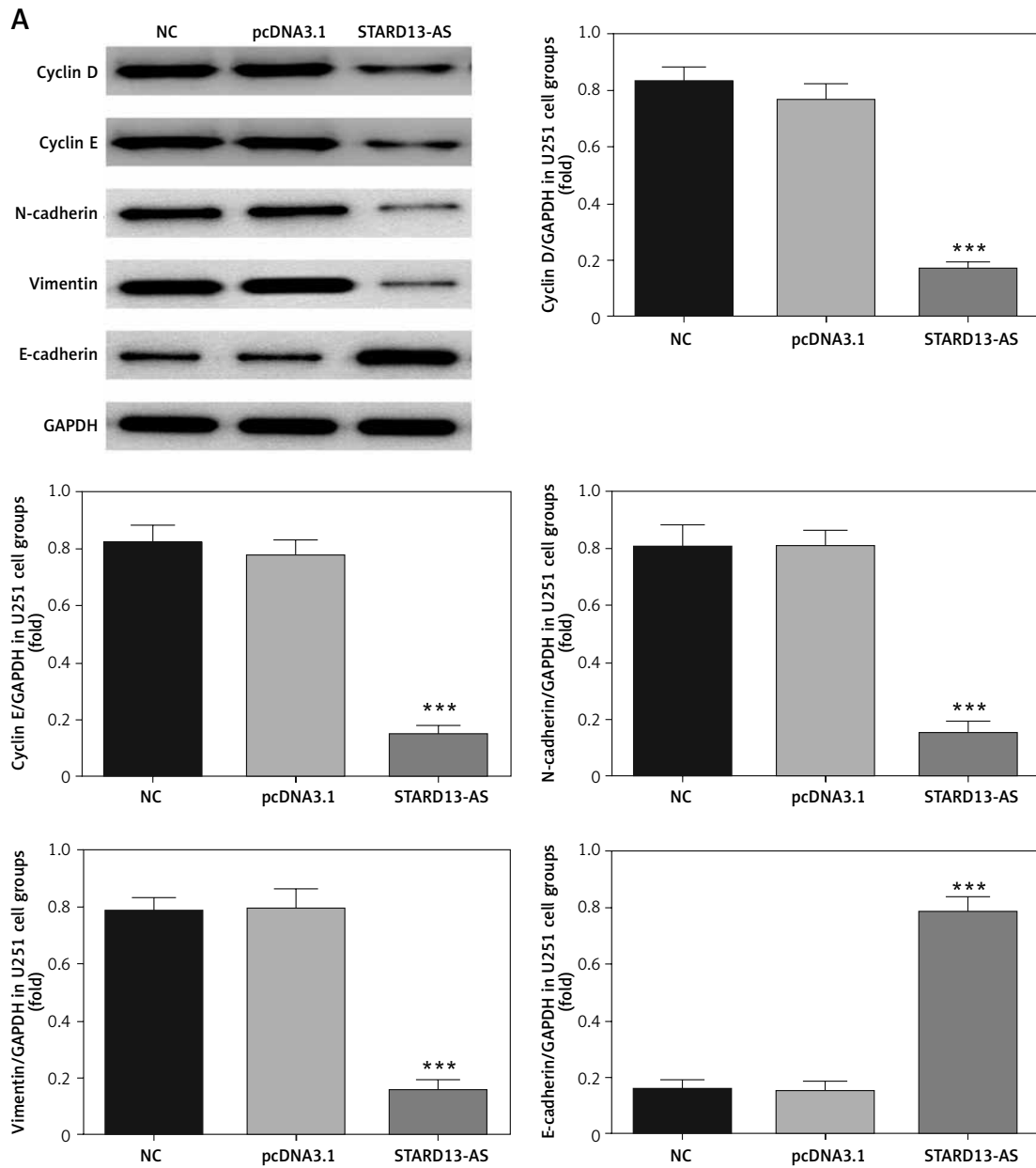
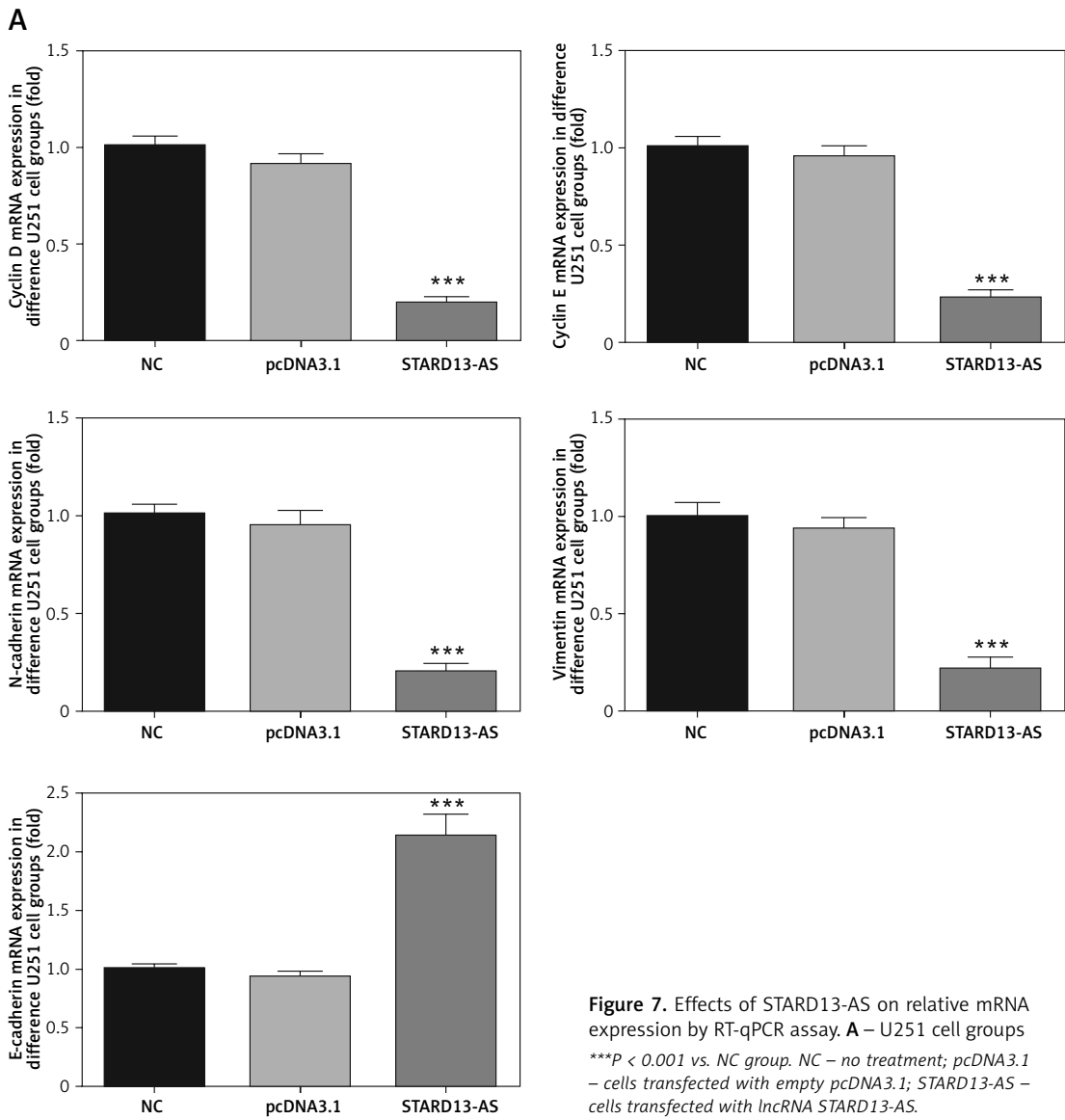**Figure 6.** Effects of STARD13-AS on relative protein expression by WB assay. **A** – U251 cell groups

***P < 0.001 vs. NC group. NC – no treatment; pcDNA3.1 – cells transfected with empty pcDNA3.1; STARD13-AS – cells transfected with lncRNA STARD13-AS.

Figure 6. Cont. **B** – U87 cell groups

***P < 0.001 vs. NC group. NC – no treatment; pcDNA3.1 – cells transfected with empty pcDNA3.1; STARD13-AS – cells transfected with lncRNA STARD13-AS.

A

Figure 7. Effects of STARD13-AS on relative mRNA expression by RT-qPCR assay. **A** – U251 cell groups

***P < 0.001 vs. NC group. NC – no treatment; pcDNA3.1 – cells transfected with empty pcDNA3.1; STARD13-AS – cells transfected with lncRNA STARD13-AS.
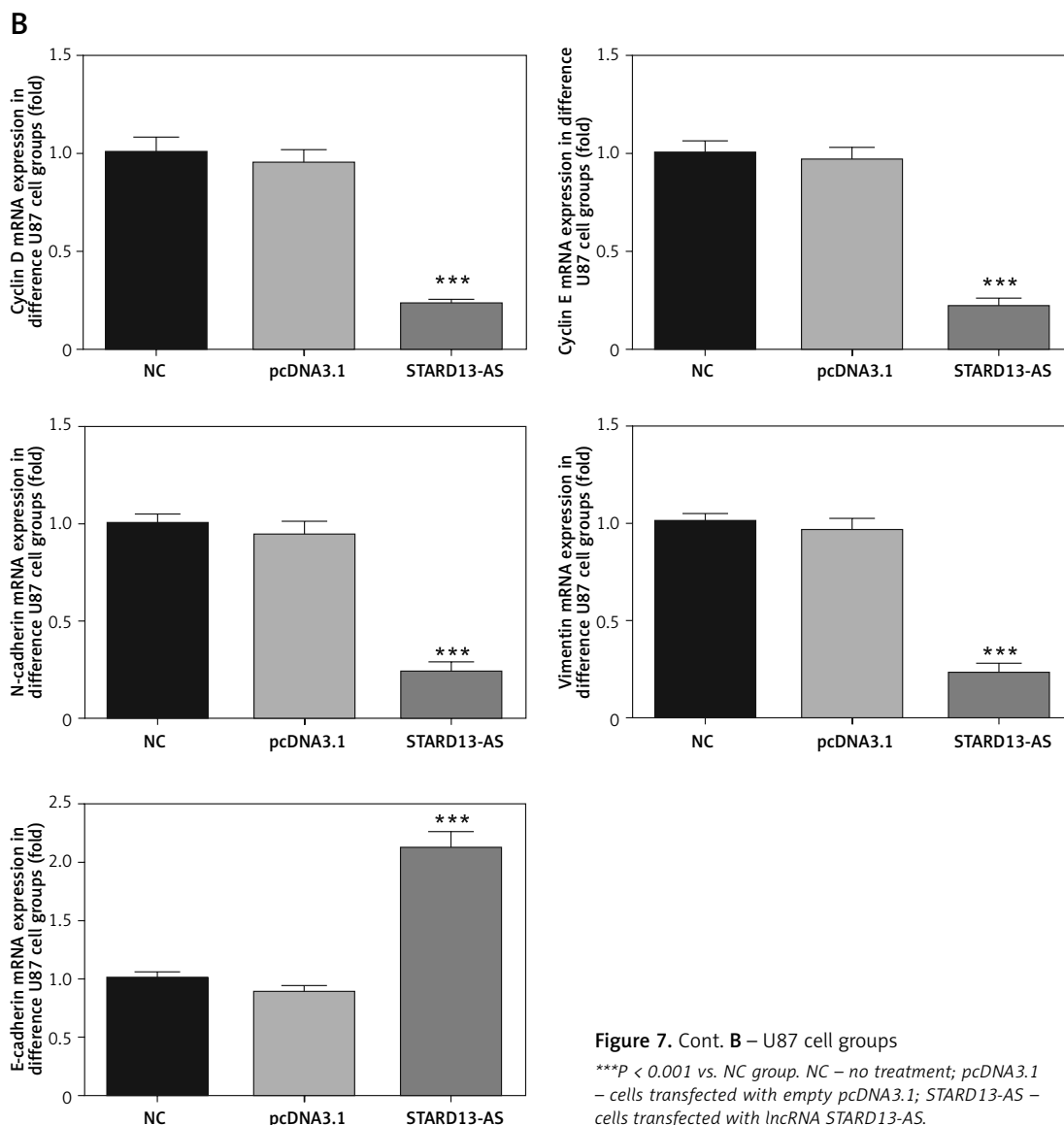
B

Figure 7. Cont. **B** – U87 cell groups

***P < 0.001 vs. NC group. NC – no treatment; pcDNA3.1 – cells transfected with empty pcDNA3.1; STARD13-AS – cells transfected with lncRNA STARD13-AS.

References

1. Tsang RW, Laperriere NJ, Simpson WJ, Brierley J, Panzarella T, Smyth HS. Glioma arising after radiation therapy for pituitary adenoma. A report of four patients and estimation of risk. Cancer 1993; 72: 2227-33.

2. Hamada K, Kuratsu J, Saitoh Y, Takeshima H, Nishi T, Ushio Y. Expression of tissue factor correlates with grade of malignancy in human glioma. Cancer 1996; 77: 1877-83.

3. Li MY, Yang P, Liu YW, et al. Low c-Met expression levels are prognostic for and predict the benefits of temozolomide chemotherapy in malignant gliomas. Sci Rep 2016; 6: 21141.

4. Kraus TF, Greiner A, Guibourt V, Lisec K, Kretzschmar HA. Identification of stably expressed lncrnas as valid endogenous controls for profiling of human glioma. J Cancer 2015; 6: 111-9.

5. Barry G. Integrating the roles of long and small non-coding RNA in brain function and disease. Mol Psychiatry 2014; 19: 410-6.

6. Hu B, Xu L, Liang D, Qi W, Fu X. LncRNA STARD13-AS expression in gastric cancer and its significance. Clin Lab 2020; 66. doi: 10.7754/Clin.Lab.2020.191261.

7. Yang B, Zhou SN, Tan JN, et al. Long non-coding RNA STARD13-AS suppresses cell proliferation and metastasis in colorectal cancer. Onco Targets Ther 2019; 12: 9309-18.

8. Li G, Guo X. LncRNA STARD13-AS blocks lung squamous carcinoma cells growth and movement by targeting miR-1248/C3A. Pulm Pharmacol Ther 2020; 64: 101949.

9. Chiang JC, Ellison DW. Molecular pathology of paediatric central nervous system tumours. J Pathol 2017; 241: 159-72.

10. Gao YF, Wang ZB, Zhu T, et al. A critical overview of long noncoding RNA in glioma etiology 2016: an update. Tumour Biol 2016; 37: 14403-13.

11. Shi J, Dong B, Cao J, et al. Long non-coding RNA in glioma: signaling pathways. Oncotarget 2017; 8: 27582-92.

12. Iyer MK, Niknafs YS, Malik R, et al. The landscape of long noncoding RNAs in the human transcriptome. Nat Genet 2015; 47: 199-208.

13. Wang Q, Zhang J, Liu Y, et al. A novel cell cycle-associated lncRNA, HOXA11-AS, is transcribed from the 5-prime end of the HOXA transcript and is a biomarker of progression in glioma. Cancer Lett 2016; 373: 251-9.

14. Gao K, Ji Z, She K, Yang Q, Shao L. Long non-coding RNA ZFAS1 is an unfavourable prognostic factor and promotes glioma cell progression by activation of the Notch signaling pathway. Biomed Pharmacother 2017; 87: 555-60.

15. Yang B, Zhou SN, Tan JN, et al. Long non-coding RNA STARD13-AS suppresses cell proliferation and metastasis in colorectal cancer. Onco Targets Ther 2019; 12: 9309-18.

16. Suk FM, Chang CC, Lin RJ, et al. Author correction: ZFP36L1 and ZFP36L2 inhibit cell proliferation in a cyclin D-dependent and p53-independent manner. Sci Rep 2019; 9: 17457.

17. Kar A, Mishra C, Biswal P, Kar T, Panda S, Naik S. Differential expression of cyclin E, p63, and Ki-67 in gestational trophoblastic disease and its role in diagnosis and management: a prospective case-control study. Indian J Pathol Microbiol 2019; 62: 54-60.

18. Rafael D, Doktorovová S, Florindo HF, et al. EMT blockage strategies: targeting Akt dependent mechanisms for breast cancer metastatic behaviour modulation. Curr Gene Ther 2015; 15: 300-12.

19. Jung HY, Fattet L, Yang J. Molecular pathways: linking tumor microenvironment to epithelial-mesenchymal transition in metastasis. Clin Cancer Res 2015; 21; 962-8.

20. Thiery JP, Acloque H, Huang RY, Nieto MA. Epithelial-mesenchymal transitions in development and disease. Cell 2009; 139: 871-90.

21. Liu S, Huang J, Zhang Y, Liu Y, Zuo S, Li R. MAP2K4 interacts with vimentin to activate the PI3K/AKT pathway and promotes breast cancer pathogenesis. Aging 2019; 11: 10697-710.

22. Rai KH, Ahmed J. A correlative study of N-cadherin expression with different grades of oral squamous cell carcinoma projecting as a marker of epithelial to mesenchymal transition in tumor progression. Asian Pac J Cancer Prev 2019; 20: 2327-32.